The final publication is available at

https://doi.org/10.1016/j.compbiomed.2022.105477

Additional Information

Characterization of tissue damage and egg viability in *C. elegans* by multispectral imaging: effect of alkaline hypochlorite in the synchronisation process

Samuel Verdú, Cristina Fuentes, José M. Barat, Raúl Grau

Departamento de Tecnología de Alimentos. Universitat Politècnica de València, Spain

*Author for correspondence: Samuel Verdú

Address: Edificio 8E - Acceso F – Planta 0

Ciudad Politécnica de la Innovación

Universitat Politècnica de València

Camino de Vera, s/n

46022 VALENCIA – SPAIN

E-mail: saveram@upvnet.upv.es

Abstract

Multispectral imaging represents powerful technique to maximizing data collection and analysis for biological materials. It improves exploitation and understood of *in vivo/vitro* experiments. This work focused on test the capability of multispectral imaging to characterize the tissue damage produced by alkaline hypochlorite on the body and eggs of the biological model *C. elegans.* To that end, three synchronisation processes differing in the final bleach and sodium hydroxide concentrations were carried out. The impact of the treatments was characterised by measuring egg viability and morphology, besides capturing multispectral images of both nematodes' bodies and eggs. Multispectral images were consisted of seven slices captured from different wavelength within visible/infrared spectrum, using different light-pass filters. Results showed dependence between increased alkaline hypochlorite concentration and loss of egg viability and morphology. This relationship was also observed for imaging data, which showed alterations in tissues´ transmittance for all tested wavelengths both for bodies and for eggs. In addition, localized alterations related to the diffusion of alkaline hypochlorite through anatomical orifices of nematodes were recognized. Applying multivariate methods on imaging data achieved successful characterization of tissue alterations, from which the type of treatment was predicted both for nematodes and for eggs. Moreover, the alterations registered by imaging data were also used to predict egg viability regardless of type of treatment (0.94). The high correlation observed between imaging data from nematodes and eggs with egg viability evidenced de capability of multispectral imaging to characterize the tissue damage and its possible practical application to study alterations in tissues of this biological model.

Keywords: multispectral imaging; tissue damage; damage characterisation; *C.elegans*; egg viability, multivariate analytics

1. Introduction

There exists a general assumption that animal and *in vitro* testing helps to study human safety at a vast range of chemical and physical agents. Biological models differ enough in specific areas to be rather limited for inter-species toxicological prediction, however these studies share important key for understanding a given physiological function (Taboureau et al., 2020; Yahya et al., 2021). Some examples are rats, mouse, pig, in the case of mammals, and flies, nematodes and fishes as non-mammalian models. These organisms are used to model the effects of a given compound on specific properties of a system, organ, tissue or cell line. These studies focus on evaluating the effects produced by the studied compounds in function of factors such as: molecular structures, chemical interactions, concentration, type of exposition, route of administration, etc.

The effects could be evaluated following different approaches from analytical and instrumental point of view. Thus, measured dependent variables depend on the type of data required to the study. Chemical and biochemical indicators, genomics, proteomics and metabolomics data, morphological data and even behavioural patterns are some of the widely worked variables. Overall, maximizing data collection and analysis of this variables during experiments represent powerful approach which could improve exploitation and understood of results. It is feasible by applying techniques and instruments which collect large amount of information from which advanced data analytics could be applied, in addition to reduce time and costs of analysis.

According to that aim, digital imaging analytics represent an extensive family of techniques which enhance the study of physicochemical impact on organisms, tissues or cells, produced by different causes. Imaging technologies are able to collect large amount of data from samples depending of the principle in which was based. Yaghini et al. (2018) applied imaging of QD photoluminescence to elucidate the in vivo toxicity of the nanoparticles in rats. Wang et al. (2020) reported laser speckle imaging as technique to study cortical cerebral bloodflow dynamics during craniotomy in rats. Rodrigues et al. (2011) study in vivo the toxicity of several compound on the structural and morphological properties of mitochondria by visualizing NADH by fluorescence imaging. Fluorescence of particles has been also used to modelling the incorporation and excretion kinetics

of mesoporous silica particles in *C.elegans* using imaging analysis (Verdú et al., 2021). Within imaging techniques, spectral imaging (multispectral/hyperspectral) represent one of the most powerful approach which is capable of capture spectral information along all coordinates within images. A spectrometer works by detecting substances that reflect/transmit specific wavelengths in a unique point. Unlike spectrometer, multispectral images assign positional data to the collected spectral information. Therefore, a multispectral images do not output a 2D information, but instead a data cube or image cube (X: image width; Y: image length; Z: wavelength) (Galeano et al., 2020; Verdú et al., 2017). This type of imaging led to the detection of amyloidopathy in Alzheimer's mouse retina, detection of cerebral ischemia in rats using hyperspectral imaging (Fu et al., 2020) or identification of microplastics and nanoplastics in vivo with nematodes *Caenorhabditis elegans* (Nigamatzyanova & Fakhrullin, 2021), proving its capacity to characterize alterations in biological materials due to different causes. In accordance with reported capacities of spectral imaging, this work focused on test the capability of multispectral imaging to characterize tissue damage produced, in this case, by chemical agents bleach and sodium hydroxide (alkaline hypochlorite) studied on the biological model *C. elegans*. The ability to rapid growth, transparency, a rapid-life cycles (3 days), and facile and inexpensive maintenance in the laboratory make this nematode a useful biological model to study the impact of physicochemical agents in specific physiological and morphological properties (Gonzalez-Moragas et al., 2015). In this regard, alkaline hypochlorite are commonly used in the synchronisation procedure during research with *C.elegans*. Synchronisation procedures aim to optimize the obtention of a sufficient number of nematodes at the same larval stage for avoiding variance generated because age differences among individuals. The alkaline hypochlorite function is to damage and dissolve tissues of gravid nematodes without damaging their eggs, whose tissues are more resistant to treatment than the nematodes´ body. In theory, each egg evolves into a synchronized nematode, however, excessive exposition to alkaline hypochlorite because handling variations produces damage in egg tissues which reduce the population viability. This common fact could produce setbacks and problems that interfere with the expected course of an experiment. Thus, this work focused on test the capability of multispectral imaging to characterize tissue damage produced by

alkaline hypochlorite on nematodes body and eggs in order to classify different tissue damage levels and then predict eggs viability.

2. Material and methods

2.1 Experimental procedure

The experiment focused on testing the capability of multispectral imaging to collect useful data from nematode´s body and eggs tissues in order to obtain information about alterations and damage because the exposition to a given substance. In this case, damage produced by alkaline hypochlorite solutions during synchronisation process were characterised. The approach was to correlate imaging data from treated nematode´s body and eggs with increasing concentration of oxidants and classifying individually eggs into viable and non-viable. Figure 1 shows the scheme of the procedure. The synchronisation process of nematodes was carried out using three solutions differing in the final sodium hydroxide and bleach concentrations (Figure 1-1). During process, nematode dispersions were stirred or non-stirred depending if whole bodies or eggs were to be studied. After procedure, samples were manually placed onto agar to capture the transmittance of tissues with multispectral images (Figure 1-2). Multispectral images were formed by a stack of seven slices captured from different light wavelength filters within visible/infrared range of electromagnetic spectrum. Viability and morphology of eggs obtained from each treatment were determined (Figure 1-3). In the other hand, samples were analysed individually by extracting regions of interest (ROIs) from multispectral images (Figure 1-4). Intensity longitudinal profiles in grayscale were extracted from each sample. Those data were used to calculate attenuation of light for each pixel across tissues with the Beer-Lambert law (Figure 1-5). Transmittance spectra from each wavelength were concatenated to obtain a unique spectrum collecting all them (Figure 1-6). Finally, imaging data was analysed by multivariate statistics to determine the capability of imaging data to differentiate treatments in conjunction of egg viability data (Figure 1-6).
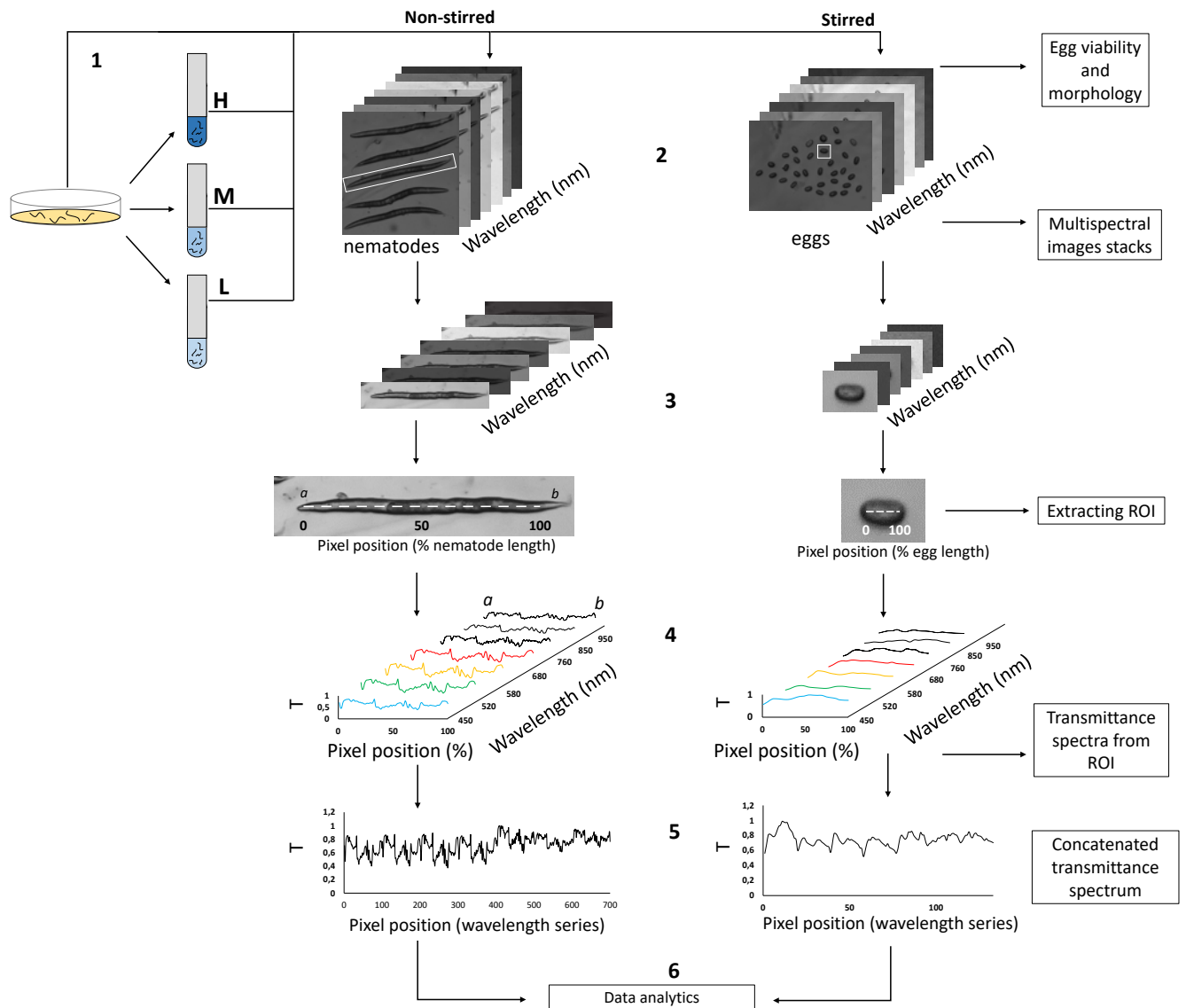
Figure 1. Experimental procedure

2.2 *C.elegans* **preparation**

Wild-type *Cahenorabditis elegans* Bristol strain N2 was employed as the object of study in this

work. The population of nematodes were reproduced on nematode growth medium (NGM) plates

seeded with *E. coli* OP50 at 20ºC (Brenner, 1974).

2.3 *C.elegans* **synchronisation method**

The synchronisation process was carried out using three solutions differing in the final sodium hydroxide and bleach concentrations (Table 1). Alkaline hypochlorite solutions were selected starting from previously reported concentrations (Porta-de-la-Riva et al., 2012).

The protocol used was the same for all the experiments. Worms were grown in 100 mm plates until adult stage. Then, plates were washed with 2-3 mL of M9 buffer and nematodes recovered into 15 mL falcon tubes. After centrifugation (1500 rpm, 1 min), the supernatant was removed and 5 mL of bleach solution were added to each tube. Tubes were vigorously shaken for 3 min and then the bleaching reaction was stopped by adding 10 mL of M9 buffer. Tubes were centrifuged again, and the pellet washed with 10 mL of M9 buffer. The washing step was repeated three times in order to completely remove the bleaching solution. Finally, eggs were placed on 55 mm NGM (0.3 mm thickness) plates without food where imaging studies were carried.

Table 1. Different alkaline hypochlorite solutions used for nematodes' synchronisation.

	L	M	H
Sodium hydroxide	0.6 M	1 M	1.6 M
Sodium hypochlorite	1 %	1.6 %	2.5 %

L: low concentration; M: medium concentration; H: high concentration

2.6 Eggs viability and morphology

The viability of the eggs was measured by counting the number of absent eggs after incubation. After extracting by synchronisation processes, eggs were manually grouped on NGM. The prepared groups of eggs were captured in the multispectral images and then incubated 24h/20ºC. After 24h, the coordinates of Petri plates with groups of eggs were captured again for counting absent samples, and therefore classify as viable due to its hatching. Figure 2-A shows an example of group of eggs captured at t=0h in a slice of multispectral image (450 nm), while Figure 2-B shows the same group after 24h, where could be observed the non-viable eggs and the marks of the viable ones (which were absent) marked in agar surface (red arrows). Viability of eggs was

expressed in % for each treatment. Synchronization processes were done per triplicate, where 350 eggs were analysed in total.
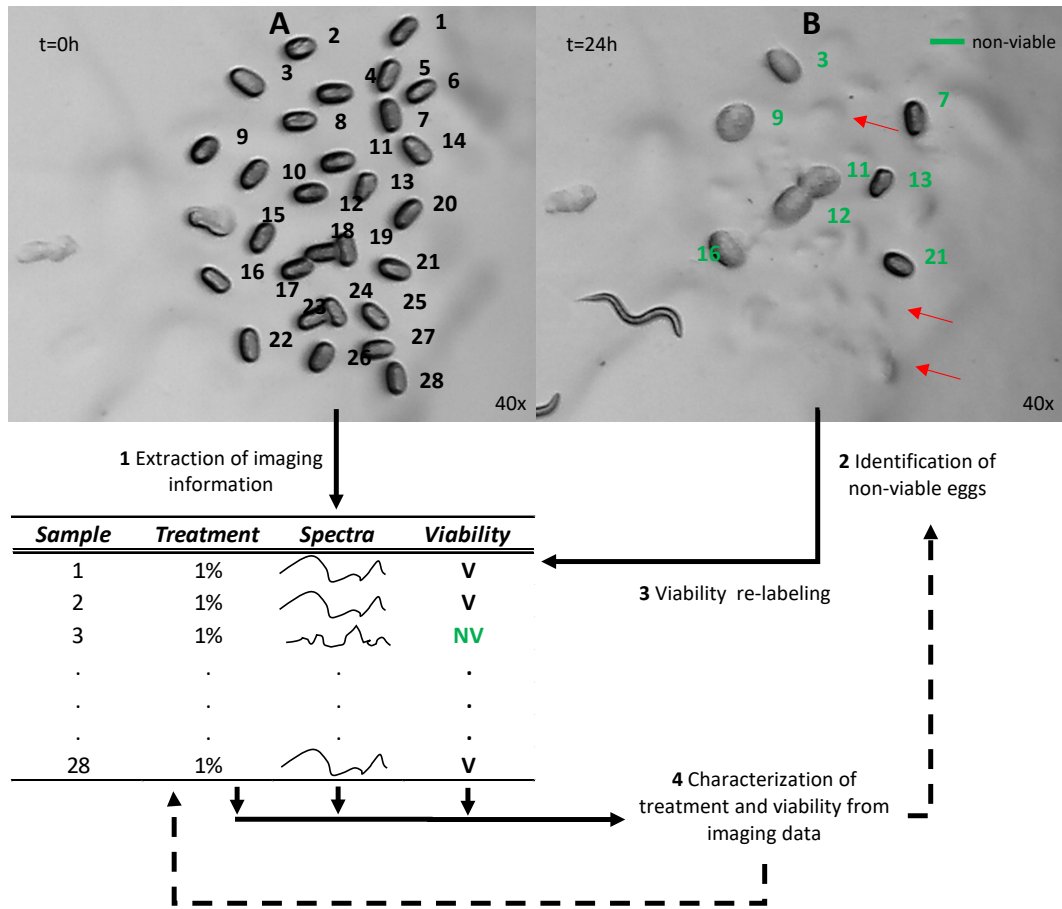

Figure 2. Example of egg viability determination and imaging processing scheme. A: eggs newly extracted after synchronization procedure. B: non-viable eggs after 24h from synchronisation procedure. V: viable egg; NV: non-viable egg.

Moreover, the shape of eggs was evaluating by calculating circularity (*C*) with imaging analysis with the aim of evaluating the effect treatments on eggshell and then better understand its relationship with multispectral response. This measurement was based on equation 1:

$$C = 4\pi \cdot \left(\frac{A}{p^2}\right)$$

(1)

Where *A* is the area and *P* is the perimeter of egg. A result of 1 indicates a perfect circle, while values trending to 0 indicates an increasingly elongated shape. This analysis was carried out using Fiji free software.

2.7 Image acquisition

After treatments, nematodes/eggs were manually placed onto NGM agar plates of 3mm thickness (Figure 1-2). Images were acquired by a Motic BA310E trinocular microscope equipped with a Moticam 3+ camera (10x, 8-bits, 2048x1536, .BMP). Seven slices (images) from different wavelengths formed multispectral images of a given field. They were obtained modifying the light source of microscope using seven different light-pass filters (Neewer®, Guangdong, China). The procedure was based on the block-based multispectral imaging registration reported by Shen et al. (2019) with modifications. The used filters were within visible-near infrared range of the electromagnetic spectra (450-520-570-650-750-850-950nm). Thus, a stack of seven images formed each multispectral image, from which data of nematodes/eggs was individually extracted. Images from 200 nematodes and 350 eggs were captured.

2.8 Image processing and data extraction

Multispectral images were used to extract information about tissues modifications calculating transmittance at each anatomic zone. It was carried out extracting an intensity profile from the region of interest (ROIs) of nematode/egg. ROI was a longitudinal line of 1 pixel width along nematode, from mouth to anus (Figure 1-4). Obtained intensity profile was discretized to 100 pixels length with the aim of comparing the spectra among samples independently of size. Pixels from 0 to 100 therefore contain the average intensity of original pixels belonging each unit. Thus, position 0 indicates mouth, while 100 indicates anus. In the case of eggs, it represented the transversal line between limits of its typical ellipsoidal shape. Intensity profile of each slice were transformed to transmittance profile by Beer-Lamber law:

$$T = \frac{I_{[0,100]}}{I_o} \qquad (2)$$

Where T was transmittance, I_o was intensity of NGM agar, while $I_{[0,100]}$ was transmitted intensity of each pixel throughout nematode/egg from positions 0 to 100. Seven transmittance profiles (one per wavelength/slice) were finally extracted from ROIs (Figure 1-5). Profiles were concatenated to get a single spectrum formed by 700 values (100 pixels x 7 wavelength) assumed as variables. Samples spectrum were collected in a multivariate matrix prepared to be analysed by multivariate statistics. Image processing was carried out with the image processing package Fiji (Schindelin et al., 2012)

2.9 Statistical analysis

The eggs viability and morphology were studied by variance study (ANOVA). In those cases in which the effect was significant (P-value < 0.05), means were compared by Fisher's least significant difference (LSD) procedure. The imaging data were explored in form of transmittance spectra and by applying multivariable statistical procedures to reduce data-matrix dimensionality. For this purpose, the multivariate unsupervised statistical method, principal component analysis (*PCA*), was employed. This method was used to reduce the dimensionality of a large set of quantitative variables (transmittance spectra) to a small number of new variables, called principal components (*PCs*), which are the result of the linear combinations of the original variables. Support Vector Machines-Discriminant Analysis (*SVM-DA*) was used to study the capability of the imaging technique to predict tissue alterations classifying nematodes/eggs by treatments. In the other hand, that procedure was also used to study the capability of the technique to classify viable/non-viable eggs, regardless of treatments. Prediction studies were done establishing randomized samples as training batch (66%) to generate the models and the remainder samples as test lot (33%) to be predicted. Results were expressed by a confusion matrix including proportions of true positives (*TP*), false positives (*FP*), true negatives (*TN*), false negatives (*FN*), from which sensitivity and specificity were calculated. These procedures were run with the PLS

Toolbox, 6.3 (Eigenvector Research Inc., Wenatchee, Washington, USA), a toolbox extension in the Matlab 7.6 computational environment (The Mathworks, Natick, Massachusetts, USA).

3. Results and discussion

3.1 Eggs viability and morphology

Results of egg viability are included in Table 2. Viability decreased with concentration of bleach/hydroxide. Control group presented 100% viability while L, M and H treatment reduced to 88.3, 63.3 and 31.4% viability respectively. Viability reduction evidenced the excessive effect of the reagents on eggs tissues for some treatments. Increasing 0.6% hypochlorite/0.4M hydroxide produced around 20% reduction in egg viability. The solvent power of reagents produced disaggregation on nematode´s body because the solution of cuticule and skin, letting eggs out of bodies. However high corrosive environment produced excessive alteration on eggshell. Thus, different degree of tissues damage was produced although the treatment time was the same.

Normally, eggshell bear the effect of bleach losing vitaline layer (VL), however excessive treatments could produce alteration in the inner layers and internal zones, which could be non-compatible with viability (Johnston & Dennis, 2012). Figure 2-B shows examples of non-viable eggs with visually detectable damage. After 24h, some of eggs did not showed visible differences with t=0, however loss of shape and texture was observed in the more extreme cases. It could be observed for the eggs 3, 9, 11, 12 and 16. Those eggs showed a loss of shape comparing to t=0, in addition to changes in optical properties. It seemed like transparent and disaggregated tissue.

Table 2. Results of egg viability and confusion matrix from prediction assays

	Treatment	Egg viability		Confusion matrix				Sensitivity	Specificity
		%	category	TP	FP	TN	FN		
Nematodes	Control			0,84	0,03	0,96	0,15	0,96	0,87
	L			0,79	0,01	0,98	0,20	0,99	0,83
	M			0,89	0,06	0,94	0,10	0,94	0,90
	H			0,93	0,08	0,92	0,06	0,92	0,94
Eggs	Control	100,0		0,97	0,01	0,99	0,02	0,99	0,98
	L	88,3		0,82	0,00	0,99	0,18	0,99	0,85
	M	63,3		0,99	0,07	0,94	0,01	0,94	0,99
	H	31,4		0,91	0,04	0,97	0,10	0,96	0,91
			viable	0,94	0,02	0,98	0,06	0,98	0,94
			non-viable	0,92	0,03	0,97	0,08	0,97	0,93

L: low concentration; M: medium concentration; H: high concentration

This phenomenon should be attributed to the abovementioned alterations on eggshell layers. Eggs have three main layers related to shape-keeping (Stein, 2018). They are vitelline layer (VL), chitin layer (CL) and chondroitin proteoglycan layer (CPGL). One function is to keep the typical ellipsoidal shape of *C.elegans* eggs, which lost when they be altered, mainly in the case of CL. CL provides the mechanical support for the egg. Thus, eggs without CL are round and misshapen (Johnston et al., 2010). Therefore, studying morphology changes from ellipsoid to cycle is a way to evidence eggshell alteration. Following that phenomenon, circularity of eggs was studied to evidence the eggshell damage. Figure 3 shows the results.
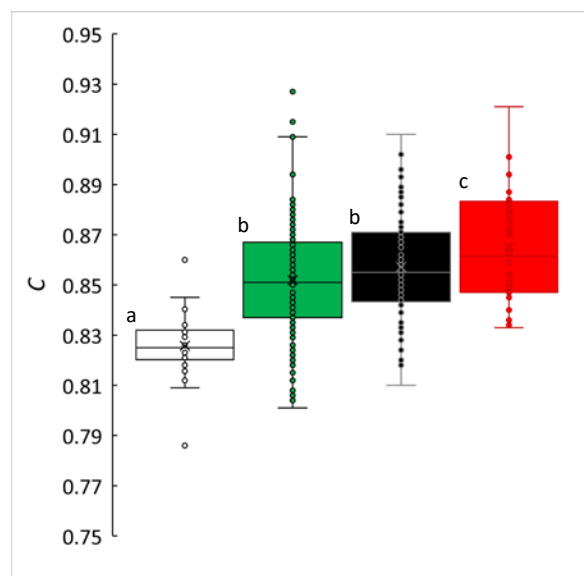

Figure 3. Results of the eggs circularity study after synchronisation treatments. Different letters indicate significant differences analysed by ANOVA ($p<0.05$). □ : Control; ■ : L; ■ : M; ■ : H.

Significant differences in circularity were observed when reagents increased. That alteration in morphology evidenced the hypothesis of tissue damage because alterations in the eggshell, which correlated with decreased eggs viability. Sodium hypochlorite is a chemical used to obtain age-synchronized nematodes because selectively removes the VL, which is not necessary in a viable egg. However, previous studies provided by Krenger et al., (2020) evidenced that the *C.elegans* eggs drastically changed the mechanical integrity because CL affectation even with a short treatment with bleach, resulting in lower resistance to puncture (Young's moduli) compared to untreated eggs. Thus, the observations matched with alterations of the CL following reagents concentration increasing. The observed eggshell alterations evidenced the effect of reagents on tissues of the studied model, which should be related with changes in optic properties of both eggs and nematodes, which should had been collected by the used imaging technique.

3.2 Imaging studies

3.2.1 Characterisation of treatments effect on nematodes

The effect of reagents concentration on the body of nematodes was evaluated analysing the transmittance spectra obtained from multispectral images, following the above explained protocol. Thus transmittance spectra of the body (the longitudinal intensity profile taken from mouth to anus) was the unit of study. Figure 4-A shows the average of transmittance spectra for each treatment and wavelength.

Results showed differences in transmittance among image slices, principally between visible and infrared blocks. Spectra from infrared slices seemed trending to higher transmittance. Moreover, in despite of differences in transmittance between slices, increasing reagents concentration raised transmittance for all them. Spectra from control group could be observed down of the rest (dotted line), while the rest placed in upper zones. Nematodes showed a common increasing of transmittance with increase of reagents concentration; however this phenomenon was not constant

along the bodies length. Differences in transmittance within bodies were observed in form of

peaks, which appeared in specific zones of the nematodes´ anatomy (black arrows in figure 3-A,
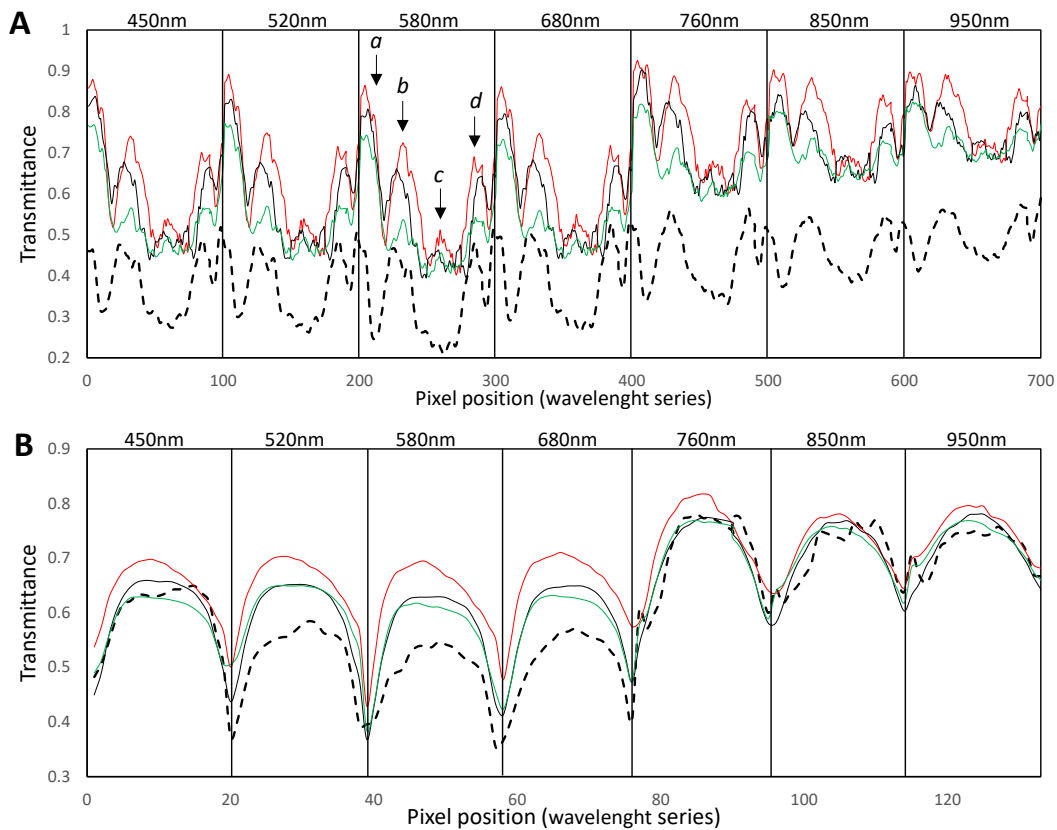
580nm).

Figure 4. Concatenated transmittance spectra extracted by multispectral imaging. A: nematode

body; B: eggs. - - Control; ▬ L; ▬ M; ▬ H. Vertical bars indicate limits of spectra within a

given slice of multispectral image corresponding to a wavelength. Letters indicate peaks related

to anatomical orifices on nematode´s body.

Four peaks were observed, which were located around specific anatomic zones where accesses in

form of orifices were naturally located. The peaks *a* and *b* were related to the oral access, the peak

c correspond to the vulva access, while the peak *d* correspond to anus. The peaks *a* and *b* should

form a single peak, however the presence of pharynx tissues increase opacity, showing a zone

with reduced transmittance between them. Transmittance showed the highest increase in that zone, following by peak *d* and *c*. It could be explained because the mouth was the unique access by which naturally penetrates fluid in suction during feed function (Corsi et al., 2015). That function increased tissues damage around that zone in such corrosive environment. Observed opacity at the pharynx zone could be related with the presence of chitin in the composition of that organ, which had higher resistance at the presence of this corrosive agents.

A scheme to understand the observed light-body interactions has been proposed in Figure 5. Alkaline hypochlorite solution is known that dissolves nematodes bodies starting with cuticle of skin and then penetrating to the rest of organs, then isolating embryos (Altun et al., 2007). Concretely, hypochlorite acting as a strong oxidant breaking the sulphide bonds of the tissue components, modifying tertiary structure of proteins and subsequently the orientation of tissue components (Esser, 1972). Thus, the observed effect of hypochlorite could arise in its corrosive activity on skin and mucous membranes (Vilesis, 1952). Previous studies reported that such phenomenon should be produced at different rates depending on reagents concentrations (Porta-de-la-Riva et al., 2012).
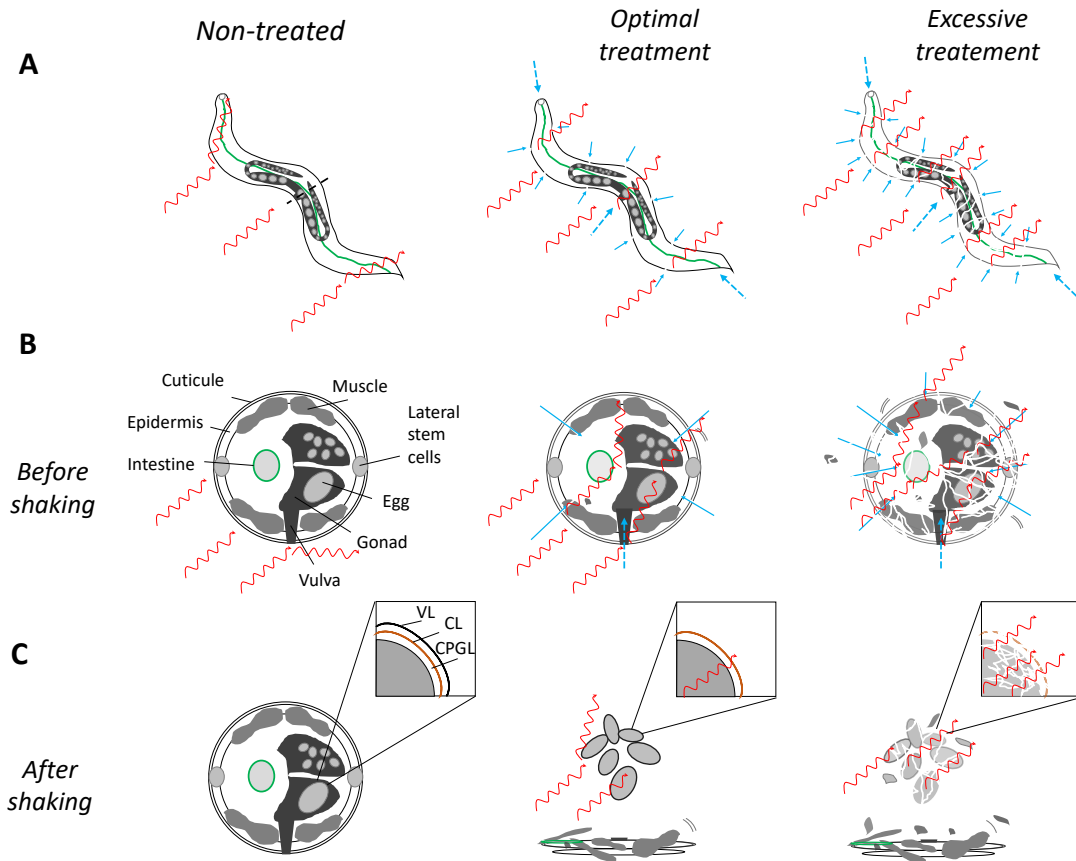
Figure 5. Tissue-light interaction for nematode and eggs at different level of treatment. A: relationship nematode damage/light/alkaline hypochlorite. B: Transversal viewpoint of relationship nematode damage/light/alkaline hypochlorite in non-shacked nematodes. C: Scheme of egg/light/hypochlorite relationship after shaking with. ➝ : alkaline hypochlorite access via anatomic orifices; ➝ : alkaline hypochlorite contact on skin; ∿ : light. VL: viteline layer; CL: chitosin layer; CPGL: chondroitin proteoglycan layer.

Therefore, increasing transmittance of bodies (Figure 4-A; 5-A) should explained increasing tissue damage due to differences in the pass of light because partial dissolution of tissues. Then, the observed peaks should indicate highly damaged zones due to an additional effect produced by alkaline solution filtered to internal surface of body by abovementioned orifices. Some images

(slice 580nm) were included in the Figure 6-A with the aim of evidencing the proposed scheme

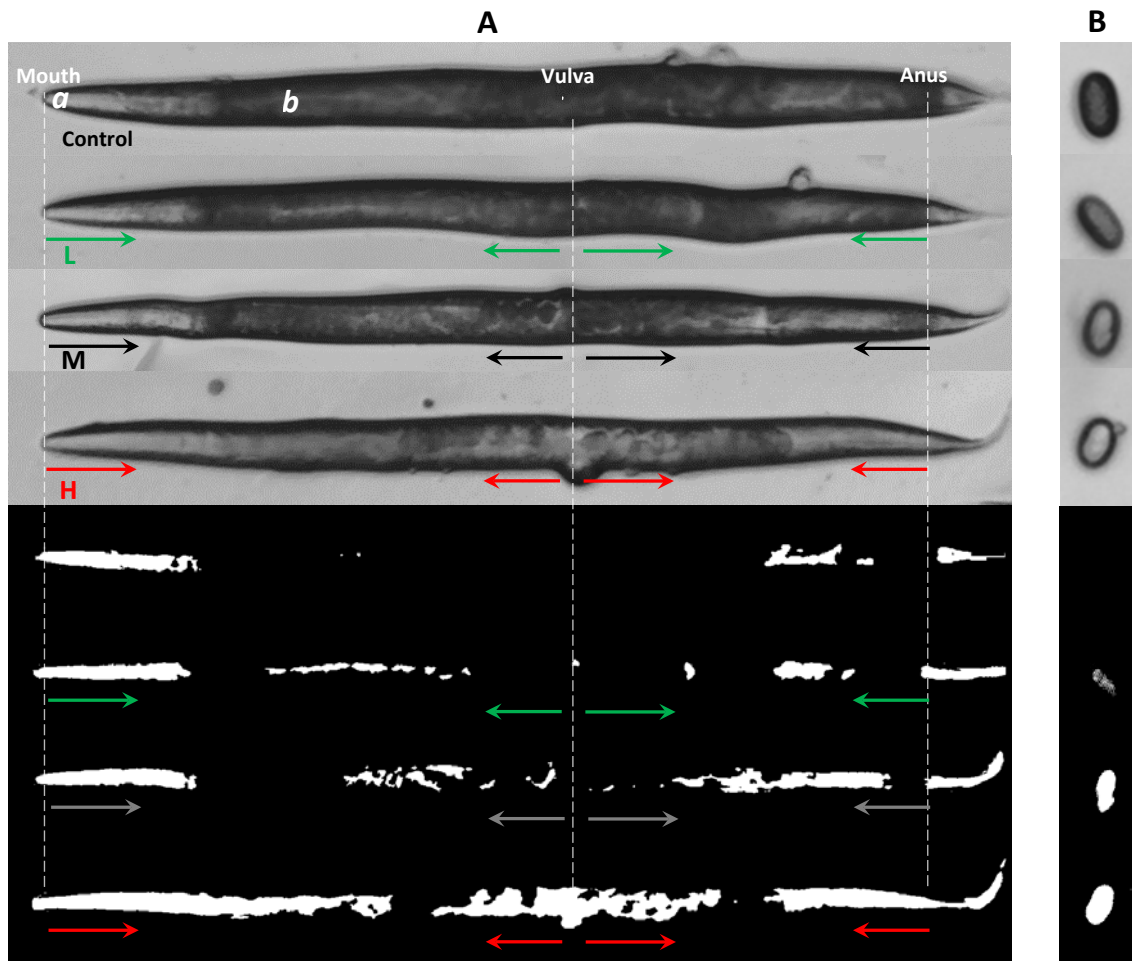in Figure 5 by observing real modifications in the nematode's anatomy.

Figure 6. Real images of treated nematodes before shaking and eggs. A: treated nematodes before

shaking. B: extracted eggs after treatment. Up: real image of treated nematodes from multispectral

slice 540nm. Down: binary image after segmentation (thresholded 93-255 grey value). Vertical

discontinuous lines indicate anatomical orifices. L: low concentration; M: medium concentration;

H: high concentration. Arrows indicate proposed direction of alkaline hypochlorite access through

anatomical orifices. — L; — M; — H. Letters indicate peaks related to anatomical orifices on

nematode´s body observed in Figure 4.

Nematodes showed observable increasing transparency following alkaline hypochlorite concentration. The zones corresponding to peaks in transmittance spectra (marked with coloured arrows) showed progressive reduction in opacity. It could be attributed to a progressive access of alkaline hypochlorite throughout the internal system, modifying tissues towards marked directions. A segmented image of the nematodes (thresholded at 93-255 grey-value) has been included at the bottom part of Figure 4-A. It was included with the aim of visualizing the areas with increased transmittance related to peaks observed in the spectra.

The segmented areas (white areas) fit the above-proposed directions of damaging and helped to explain the observed shapes in the transmittance spectra. Thus, results allowed us to observe two possible effects of alkaline hypochlorite during treatments. On the one hand, it noted a generalized increased transmittance of body tissues with reagents concentration, which was principally produced by the alterations undergone by skin surface. This effect principally affected cuticle of skin, whose major component is collagen. That protein represents over 80% of the soluble protein released during its exposition to these corrosive agents (Chisholm & Hsiao, 2012). Thus, the undergone corrosion promoted conditions in skin to increase light-pass such as transparency increase due to thickness reduction. Secondly, the penetration of reagents to internal zones by natural orifices produced additional damage on adjacent zones, which generated higher transmittance than the rest of the body. These two ways for tissue damaging matched with the impact of treatments in observed egg viability. This result might indicate that eggshell were already exposed to reagents previously to the extraction. The observed penetration of solution into uterus and gonad zones (peak c, Figure 4-A) could affect eggshell before direct contact with the alkaline solution after shaking (Figure 5-B; 5-C).

Based on the results visualized for nematodes, the feasibility of characterising treatment damage level on bodies from image information was explored. To this end, multivariable statistics were applied with the aim of exploiting the large amount of information provided by multispectral images. Firstly, a non-supervised study of the image data was done based on a PCA. A variance space was generated from the PC1 and PC2 (Figure 7-A), which collected 63.1% and 15.3% total

variance respectively. Data showed four nuclei matching the treatments. The position of each nuclei across PC1 scores fit with the increasing concentration of alkaline hypochlorite. It meant PC1 collected the variance generated in imaging data because the effect of reagents concentration on the optical properties of nematode body. The highest difference was for control group, which also presented less dispersion than the rest. However, although the rest of groups had major dispersion, clustering was enough to differentiate treatments.

The dependence of the imaging data to tissue damage was evidenced by PCA, even though this method was a non-supervised approach. Thus, for further deepening in the capacity of this imaging technique to discriminate different levels of tissue damage, SVM-DA was applied as method to classify nematodes by treatments. Table 2 shows the confusion matrix obtained from classification studies using transmittance spectra data of nematode bodies. Both sensitivity and specificity were higher than 0.80 for all groups, with 0.99 and 0.98 for control sensitivity and minor treatment respectively. Thus, the results of the discriminant analysis showed the capability of imaging data to capture the variance generated by different levels of tissues alterations from which differentiate treatments with high precision.
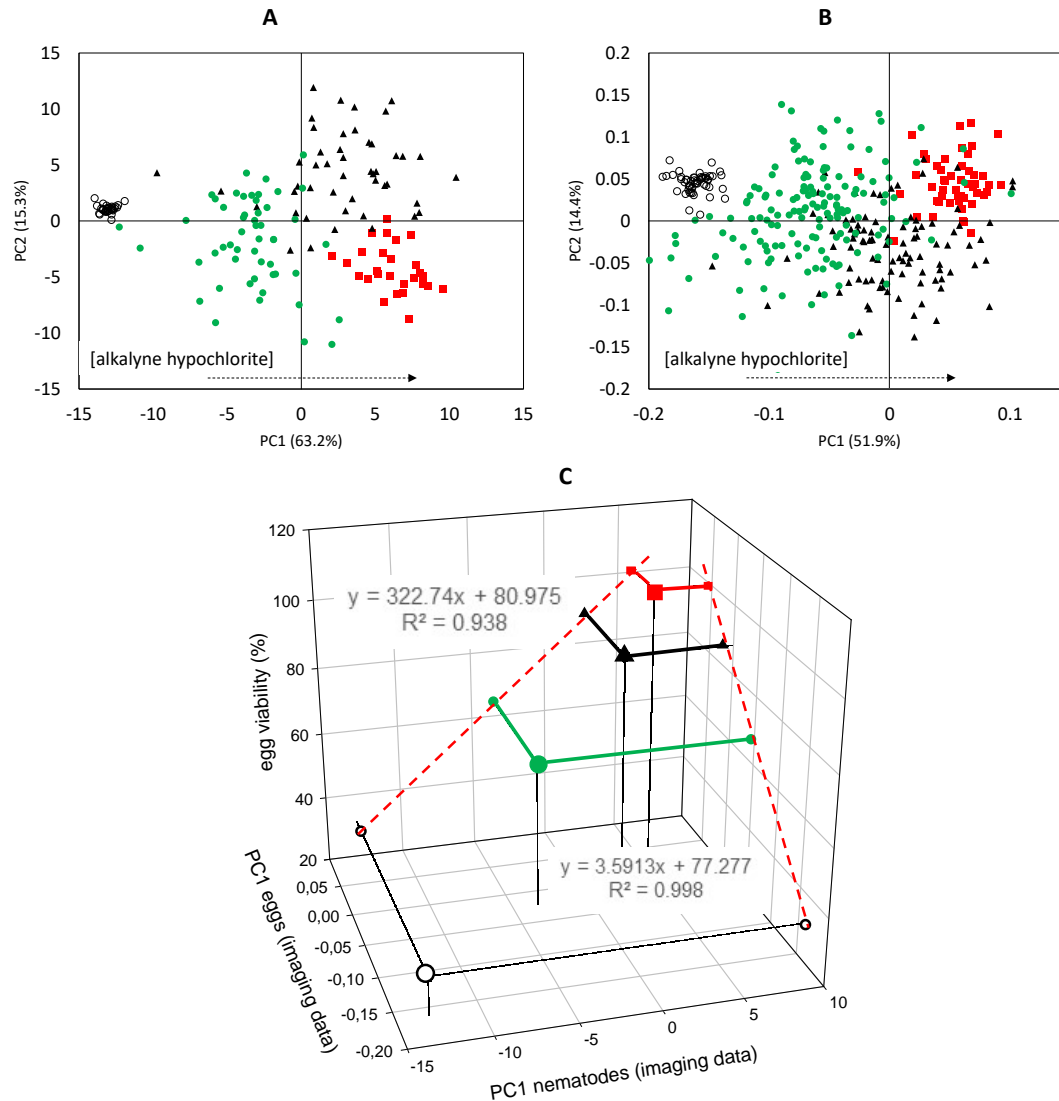
Figure 7. Characterisation of treatments from imaging data. A: PCA variance space from multispectral imaging data of nematodes. B: PCA variance space from multispectral imaging data of eggs. C: relationship between imaging data from both types of samples and egg viability.

- - Control; ▬ L; ▬ M; ▬ H; - - regression imaging data vs. egg viability.

3.2.2 Characterisation of the treatments effect on eggs

After to observe the relationship between alkaline hypochlorite effect on nematode body and egg viability, imaging technique was applied to study the impact of alkaline hypochlorite concentration in optic properties of eggs. In the same way of the study on nematodes, the aim was

to characterize tissue damage undergone during treatments. Figure 4-B shows the average transmittance profiles for eggs from each treatment. The effect of alkaline hypochlorite on transmittance was parallel to the nematodes, however in this case anatomic differences could not be identified because the homogeneous egg structure itself. In this case spectra showed curved shape due to the natural ellipsoid morphology of the eggs. The parallelism with nematode spectra fall on that egg tissue also increased transmittance with concentration for all wavelength, although in this case, the infrared zone had the lower differences compared to the control group. These findings were consistent because, despite of the eggshell is known that should resist moderate bleach treatment losing VL, the rest of layers could be also damaged under an excessive treatment. Thus, increase of transmittance seems to be also produced by reducing layers thickness of eggshell and then allowed major light-pass (Figure 5-C). This plausible layer's damage fit with the observed loss of morphology above commented in Figure 3.

Figure 6-B shows eggs from each treatment and the segmented version of the original images. The effect on egg opacity was visually lower, however a generalized increase of transparency could be also observed.

In this case, a similar evolution to nematodes data was observed when imaging data of eggs was analysed by PCA. Figure 7-B shows the variance space generated by PC1 and PC2, which collected 51.9% and 14.4% total variance respectively. Samples were grouped following increase of alkaline hypochlorite across PC1. In the same way to nematodes, control group presented the lowest dispersion. That dispersion was high for the three treatments because the non-supervised approach of PCA provided maximum variance among samples regardless the categories, however when the classification method was applied, results were significantly improved. Thus, when SVM-DA was applied, high sensitivity and specificity coefficients were obtained to differentiate treatments (Table 2). The highest sensibilities were found to control and L treatment with 0.99. In the case of specificity, M treatment had the maximum with a 0.98.

These results evidenced the dependency of imaging data variance from the impact of alkaline hypochlorite in tissues for both nematode body and eggs. Evolution of imaging data from both

nematodes and eggs matched with egg viability, therefore, the relationship among damage on nematodes and eggs with egg viability was evidenced. That relationship could be observed when data from that three variables was represented. Figure 7-C shows a 3D plot where average PC1 scores from imaging studies of nematodes and egg studies were related with % egg viability. Result showed direct proportionality of imaging data with egg viability. Imaging data from eggs correlated with egg viability with $R^2=0.938$, while the imaging data from nematodes had $R^2=0.998$. Thus, based on those correlations, the possibility of using imaging data from eggs to predict the viability itself was explored within the range of the studied alkaline hypochlorite concentrations.

3.2.3 Prediction of egg viability

To study the possibility to know the viability of eggs regardless of their synchronisation treatment, once the capacity of imaging technique to characterising damage in eggs was evidenced, the probability of individual discrimination between viable and non-viable eggs was tested based on the same imaging dataset. In this case, the samples were divided into two groups: viable and non-viable eggs, regardless the treatment used to extract them. This study was done under the premise that viability of an egg after synchronisation process depended on the damage level produced by alkaline hypochlorite. It was based on the fact that, excepting the control group, all treatments produced non-viable eggs in different percentage. Thus, SVM-DA was applied to study the capability of the imaging technique to individually identification between viable/non-viable eggs. Results in sensibility and specificity terms are included in Table 2.

Non-viable eggs group was successfully discriminated with 0.93 specificity, while 0.98 as maximum sensitivity for the viable eggs group. Results showed the capacity of imaging data to collect the variance generated by treatments in eggs tissues until make them non-viable. It means that captured variance by imaging technique contained information to differentiate both among treatments and detect viability of each egg. Therefore, the prediction of individual viability of

eggs could be carried out from imaging dataset with independence of treatment intensity. These results confirm the possibility of using multispectral imaging as tool to characterizing chemical damage in tissues of this type of biological models.

4. Conclusions

The capacity of multispectral imaging to characterize tissue damage in body and eggs of the biological model *C.elegans* during synchronisation process was tested. Increasing alkaline hypochlorite concentration during process reduced egg viability. This reduction was related with an excessive treatment that dissolved chitin layer of eggs, evidenced by loss of original egg-shape after morphological analysis. Imaging data was capable to collect variance generated in optical properties of nematodes because different levels of tissue alteration. These results showed generalized increase in transmittance along nematodes´ tissues and eggs following the rise of alkaline hypochlorite concentration. On the other hand, increased tissue alteration was recognized in specific zones due to the penetration of alkaline hypochlorite throughout the anatomical orifices: mouth, vulva and anus. Exploration of imaging data by means of non-supervised multivariate statistics evidenced quantitative registration of damage level by the technique. It evidenced the alteration of optical properties of tissues and its relationship with treatment intensity. Such relationship made it possible to perform well prediction of treatment type both for nematodes and eggs. The dependence of imaging data from treatments evidenced the capability of multispectral imaging to characterize tissue alteration in this biological model because the effect of a chemical agent, in this case. Results suggest the possibility of applying this imaging technique as a tool to improve the study of tissue alterations in *C.elegans*. In future works, the next step should extend the number of wavelengths both from visible and infrared range. Furthermore, the capability to characterize impact of other compounds on the studied tissues should be taken into account to develop a possible device.

5. Acknowledgments

6. Bibliography

Altun, Z. F., Herndon, L. A., Norris, C., Xu, M., Crocker, C., Stephney, T., & Hall, D. H. (2007). WormAtlas and WormImage: The Websites and the Book. In *International Worm Meeting*.

Brenner, S. (1974). The genetics of Caenorhabditis elegans. *Genetics*.

Corsi, A. K., Wightman, B., & Chalfie, M. (2015). A transparent window into biology: A primer on Caenorhabditis elegans. *Genetics*, *200*(2), 387–407. https://doi.org/10.1534/genetics.115.176099

Esser, R. P. (1972). Effect of Sodium Hypochlorite Concentrations on Selected Genera of Nematodes. *Proc. Helm. Soc. Wash.*, *39*(1), 108–114. http://bionames.org/archive/issn/0018-0130/39/108.pdf

Fu, C., Ma, K., Li, Z., Wang, H., Chen, T., Zhang, D., Wang, S., Mu, N., Yang, C., Zhao, L., Gong, S., Feng, H., & Li, F. (2020). Rapid, label-free detection of cerebral ischemia in rats using hyperspectral imaging. *Journal of Neuroscience Methods*. https://doi.org/10.1016/j.jneumeth.2019.108466

Galeano, J., Zarzycki, A., Garzón Reyes, J., & Moncada, M. E. (2020). Optical characterization of collagen scaffolds using multispectral images and a light-scaffold interaction model. *Biomedical Signal Processing and Control*, *62*. https://doi.org/10.1016/j.bspc.2020.102087

Gonzalez-Moragas, L., Roig, A., & Laromaine, A. (2015). C. elegans as a tool for in vivo nanoparticle assessment. *Advances in Colloid and Interface Science*, *219*, 10–26.

https://doi.org/10.1016/j.cis.2015.02.001

Johnston, W. L., & Dennis, J. W. (2012). The eggshell in the C. elegans oocyte-to-embryo transition. *Genesis*, *50*(4), 333–349. https://doi.org/10.1002/dvg.20823

Johnston, W. L., Krizus, A., & Dennis, J. W. (2010). Eggshell chitin and chitin-interacting proteins prevent polyspermy in C. elegans. *Current Biology*, *20*(21), 1932–1937. https://doi.org/10.1016/j.cub.2010.09.059

Krenger, R., Burri, J. T., Lehnert, T., Nelson, B. J., & Gijs, M. A. M. (2020). Force microscopy of the Caenorhabditis elegans embryonic eggshell. *Microsystems and Nanoengineering*, *6*(1). https://doi.org/10.1038/s41378-020-0137-3

Nigamatzyanova, L., & Fakhrullin, R. (2021). Dark-field hyperspectral microscopy for label-free microplastics and nanoplastics detection and identification in vivo: A Caenorhabditis elegans study. *Environmental Pollution*. https://doi.org/10.1016/j.envpol.2020.116337

Porta-de-la-Riva, M., Fontrodona, L., Villanueva, A., & Cerón, J. (2012). Basic Caenorhabditis elegans methods: Synchronization and observation. *Journal of Visualized Experiments*, *64*, 1–9. https://doi.org/10.3791/4019

Rodrigues, R. M., Macko, P., Palosaari, T., & Whelan, M. P. (2011). Autofluorescence microscopy: A non-destructive tool to monitor mitochondrial toxicity. *Toxicology Letters*, *206*(3), 281–288. https://doi.org/10.1016/j.toxlet.2011.06.025

Schindelin, J., Arganda-Carreras, I., Frise, E., Kaynig, V., Longair, M., Pietzsch, T., Preibisch, S., Rueden, C., Saalfeld, S., Schmid, B., Tinevez, J. Y., White, D. J., Hartenstein, V., Eliceiri, K., Tomancak, P., & Cardona, A. (2012). Fiji: An open-source platform for biological-image analysis. In *Nature Methods*. https://doi.org/10.1038/nmeth.2019

Shen, H. L., Zou, Z., Zhu, Y., & Li, S. (2019). Block-based multispectral image registration with application to spectral color measurement. *Optics Communications*, *451*(February), 46–54. https://doi.org/10.1016/j.optcom.2019.06.041

Stein, K. K. (2018). The C. elegans eggshell. *WormBook*, 1–36.

    https://doi.org/10.1895/wormbook.1.179.1

Taboureau, O., El M'Selmi, W., & Audouze, K. (2020). Integrative systems toxicology to

    predict human biological systems affected by exposure to environmental chemicals.

    Toxicology and Applied Pharmacology, *405*, 115210.

    https://doi.org/10.1016/j.taap.2020.115210

Verdú, S., Ruiz-Rico, M., Barat, J. M., & Grau, R. (2021). Evaluation of the influence of food

    intake on the incorporation and excretion kinetics of mesoporous silica particles in

    C.elegans. *Chemico-Biological Interactions*, *334*(December 2020).

    https://doi.org/10.1016/j.cbi.2020.109363

Verdú, S., Vásquez, F., Ivorra, E., Sánchez, A. J., Barat, J. M., & Grau, R. (2017).

    Hyperspectral image control of the heat-treatment process of oat flour to model composite

    bread properties. *Journal of Food Engineering*, *192*, 45–52.

    https://doi.org/10.1016/j.jfoodeng.2016.07.017

VILEISIS, C. (1952). Black widow spider bite. *Delaware Medical Journal*, *24*(6), 159–162.

Wang, C., Xian, L., Chen, X., Li, Z., Fang, Y., Xu, W., Wei, L., Chen, W., & Wang, S. (2020).

    Visualization of cortical cerebral blood flow dynamics during craniotomy in acute

    subdural hematoma using laser speckle imaging in a rat model. *Brain Research*,

    1742(April), 146901. https://doi.org/10.1016/j.brainres.2020.146901

Yaghini, E., Turner, H., Pilling, A., Naasani, I., & MacRobert, A. J. (2018). In vivo

    biodistribution and toxicology studies of cadmium-free indium-based quantum dot

    nanoparticles in a rat model. *Nanomedicine: Nanotechnology, Biology, and Medicine*,

    14(8), 2644–2655. https://doi.org/10.1016/j.nano.2018.07.009

Yahya, F. A., Hashim, N. F. M., Israf Ali, D. A., Chau Ling, T., & Cheema, M. S. (2021). A

    brief overview to systems biology in toxicology: The journey from in to vivo, in-vitro and

–omics. In *Journal of King Saud University - Science* (Vol. 33, Issue 1, p. 101254).

Elsevier B.V. https://doi.org/10.1016/j.jksus.2020.101254